

Worst-Case Crosstalk Noise for Non-Switching Victims in High-speed Buses

Jun Chen and Lei He
Electrical Engineering Department,
University of California, Los Angeles

Abstract— Considering RLC interconnect model, we determine switching patterns and switching times of multiple aggressors to generate the worst-case crosstalk noise (WCN) for a quiet or a noisy victim. We consider the routing direction as it has a significant impact under RLC model. When there are no timing window constraints, we show that the commonly used superposition algorithm results in 15% underestimation on average, and propose a new $SS+AS$ algorithm that has virtually the same complexity as the superposition algorithm but has a much improved accuracy. On average the $SS+AS$ algorithm only underestimates WCN by 3% compared to time-consuming simulated annealing and genetic algorithm. We also shows that applying RC model to the high-speed interconnects in the ITRS $0.10\mu m$ technology virtually always underestimates WCN, and the underestimation can be up to 80%. Furthermore, we extend our algorithm to consider aggressor switching windows and the victim sampling window. We show that the extended $SS+AS$ algorithm well approximates WCN with 2% underestimation on average. Although RC model usually severely underestimates WCN with timing window constraints, it *does* overestimate when both the aggressor switching windows and the victim sampling window are small enough. We conclude that RLC model is needed for accurate modeling of WCN in design in multi-gigahertz region.

I. INTRODUCTION

The coupling induced crosstalk noise gains growing importance in deep-submicron circuits and systems with higher clock frequency. Crosstalk noise may cause variation of delay and logic failure of a victim net. The worst-case delay (WCD) defined as the maximum possible delay caused by crosstalk noise has been studied in [1] and [2] under RC model, and the worst-case noise (WCN) defined as the maximum possible crosstalk noise has been studied in [3]. In [3], it is assumed that driver and receiver sizes, wire spacing, and net ordering are given, and interconnects can be modeled by distributed RC circuits. The WCN problem is formulated as finding the alignment of switching times for multiple aggressors such that WCN is reached.

As we move to multi-gigahertz designs, the inductive crosstalk noise can no longer be ignored [4], [5]. With the consideration of inductance, the WCN problem becomes much

more complicated. We need to consider (i) switching pattern generation in addition to the alignment of switching times for multiple aggressors, as the same direction switching assumed for the WCN problem under RC model does *not* always lead to WCN under RLC model; (ii) coupling between both adjacent and non-adjacent interconnects, while the WCN problem under RC model only takes into account coupling between adjacent interconnects; and (iii) routing direction of signal wires. It is defined as whether the signal is routed from left (top) to right (down) or vice versa, and has a significant impact on WCN under RLC model.

Assuming RLC interconnect model and multiple switching aggressors, in this paper we study the problem of switching pattern generation and switching time alignment leading to WCN at the far-end of a quiet or a noisy victim, with the consideration of the aggressor switching time windows and the victim sampling time window as well as the signal routing direction. The rest of the paper is organized as follows: In section II, we review the WCN problem formulation and algorithms under RC model, and discuss the characteristics and formulation of the WCN problem under RLC model. In section III, we present the algorithms and experiment results for the WCN problem under RLC model without timing window constraints. We extend our algorithms to the WCN problem with timing window constraints in section IV. Finally, we conclude our paper in section V.

II. PRELIMINARIES AND PROBLEM FORMULATION

A. Interconnect and device models

We study the interconnect structure with one victim wire (in short, the victim) and multiple aggressor wires (in short, the aggressors). A victim is *quiet* when there is no signal/noise propagated from its previous stage, it is *noisy* when the signal/noise propagated from the previous stage is less than the logic threshold, and it is *switching* otherwise. In this paper, we study WCN only for non-switching victims that are either quiet or noisy. Moreover, we assume that aggressors may have arbitrary switching patterns (i.e., switching high or switching low).

We assume that all drivers (receivers) have a uniform size, and are cascaded inverters. For the best accuracy, we use BSIM3 model [6] for the predicted ITRS $0.10\mu m$ technology to model all drivers and receivers. BSIM model is a nonlinear device model. In contrast, there are linearized device models, such as the effective switching resistance model [7] and C_{eff}

Manuscript received September 08, 2003; revised June 4, 2004 and November 07, 2004. This paper is partially supported by NSF CAREER award CCR-0401682, SRC grant 1100, a UC MICRO grant sponsored by Analog Devices, Fujitsu Laboratories of America, Intel and LSI Logic, and a Faculty Partner Award by IBM.

The authors are with the Electrical Engineering Department, University of California, Los Angeles, CA 90095 USA (e-mail: jchen@ee.ucla.edu; lhe@ee.ucla.edu).

model [8]. The effective switching resistance model uses a fixed-value resistor to model a device. Interconnects with drivers and receivers become linear circuits under this model, leading to inaccurate estimation of WCN.¹ The C_{eff} model is able to catch the device nonlinearity for a single RC or RLC tree, and has been used for the worst-case delay problem under RC model [1]. We plan to study its applicability to the WCN problem under RLC model in the future but not in this work.

Interconnects can be modeled by either RC or RLC circuits. In this work, we assume that all wires have a uniform width and spacing, and construct a π -type circuit for every $200\mu\text{m}$ long wire segment for both RC and RLC models. We only consider the coupling capacitance between adjacent wires because coupling capacitance between nonadjacent wires is negligible. For RC model, both self inductance and mutual inductance are ignored. For RLC model, we consider self inductance for each wire segment, and mutual inductance between *any* pair of wire segments, even though they may belong to the same net. Such a RLC circuit model is called full PEEC model in [9]. We use full PEEC models for all our experiments.

We carry out SPICE simulations on the RLC circuits of interconnects with BSIM models of drivers and receivers to validate our algorithms. In the following of this paper, we use predicted ITRS $0.10\mu\text{m}$ technology shown in table I. We assume that the input rising time is 33ps. We assume uniform driver size and receiver size. The driver size, wire length and wire spacing are varied and specified as needed in the experiments. Note all the drivers and receivers are cascaded inverters [10]. The receiver has two stages and the first stage is $3\times$. We measure noise at the inputs of receivers and report noise normalized with respect to VDD. It is worthwhile to point out that our algorithms can be applied to any accurate interconnect analysis methods.

TABLE I
EXPERIMENT SETTINGS

| Technology | ITRS $0.10\mu\text{m}$ |
|--------------------|------------------------|
| Signal rising time | 33ps |
| Wire thickness | $0.75\mu\text{m}$ |
| Wire width | $0.6\mu\text{m}$ |
| Receiver size | 10x |

B. WCN under RC model

If only capacitive coupling is considered, there is no resonance in the noise waveform. When an aggressor switches, there is only one noise peak on the victim with the polarity same as that of the aggressor signal. To achieve the maximum noise, all the noise peaks should have a same polarity, and so do all the aggressor signals. Therefore, the WCN problem under RC model can be simplified as the alignment of aggressor switching times to maximize the noise on the victim, without considering aggressor switching patterns.

¹Superposition achieves the accurate solution only for a linear circuit. Because the devices are not linear in nature, our experiments in section III-B will show that superposition leads to underestimation in most cases.

The following algorithms have been widely used: (i) *Simultaneous switching (SS)*: All the aggressors switch simultaneously. WCN is approximated by the maximum noise value on the victim. And (ii) *Superposition (SP)*: Find the maximum noise peak when only one aggressor switches, then approximate WCN by the sum of all such noise peaks. The *Aligned Switching (AS)* has been proposed in [3], where we find the *peak time* as the time of the maximum noise peak when only one aggressor switches, then simulate the interconnect structure with all aggressors switching at the times *aligned* according to the above peak times (see an alignment example in Figure 1). The maximum noise in the last simulation is WCN.

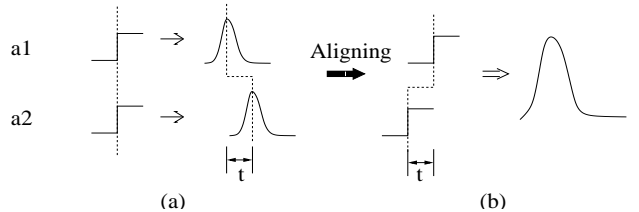


Fig. 1. Alignment operation illustrated using two aggressors. (a) We simulate the interconnects with only one aggressor switching in each simulation, and find the skew t between noise peaks. (b) We simulate the interconnects with both aggressors switching. When their switching times are aligned by t , the overall noise due to the two aggressors is likely maximized [3].

The time complexity is 1 for *SS*, n for *SP*, and $n + 1$ for *AS*, where n is the total number of aggressors and we measure the complexity in terms of the total number of simulations needed to analyze the interconnect structure. According to [3], *AS* closely approximates WCN with underestimation less than 5%, *SS* always underestimates WCN, and *SP* can severely overestimate or underestimate WCN. We will discuss how to extend *SS*, *SP* and *AS* for the WCN problem to RLC model in section III.

C. WCN under RLC model

1) *Impact of Shielding*: In this work, we assume there are shields at both edges of the bus structure under study. This assumption is realistic, because there are always power/ground wires in the same or adjacent routing layer and these wires can serve as shield wires. A few recent papers [11], [12], [13] have also proposed to insert dedicated shields to further reduce crosstalk noise. To justify the usage of shields, we have studied noise in a sixteen-bit bus structure with and without edge shields. We assume that bit-1 is the aggressor, and compute noise for quiet victims from bit-2 to bit-16 (see Figure 2). One can easily see that the noise is much smaller with presence of edge shielding wires. We assume that there are two edge shields in the bus structures studied, but do not assume that the current returns on the shields. Because we use partial inductance model, we do not need to specify the current return path and the current distribution is implicitly determined by SPICE simulations. Note our assumption of shielding does not affect the validity of our algorithms.

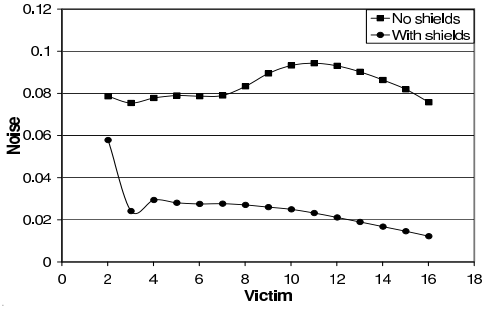


Fig. 2. Noise in a sixteen-bit $1000\mu\text{m}$ -long bus. The driver size is $200\times$, and the wire spacing is $0.6\mu\text{m}$

2) *Impact of Switching Pattern*: Different from RC interconnect model, the waveform may have resonance due to inductance under RLC model. Resonance results in multiple noise peaks with opposite polarities. It is not certain which peak is the largest. In Figure 3, we show a bus structure with two aggressors, where v is the quiet victim, q is a quiet wire, a is an aggressor, and s is a shield. We also present two waveforms, each for the noise on the quiet victim with only one of the two aggressors switching up. From the figure, either the positive or the negative peak in this example can be the larger one between the two peaks due to a same aggressor (in general, an aggressor may generate more than two noise peaks). Furthermore, WCN may happen when aggressors switch in a same direction or different directions. Such an example is shown in table II for a same bus topology but with different wire spacings. Therefore, we must consider switching pattern generation in addition to switching time alignment for WCN under RLC model.

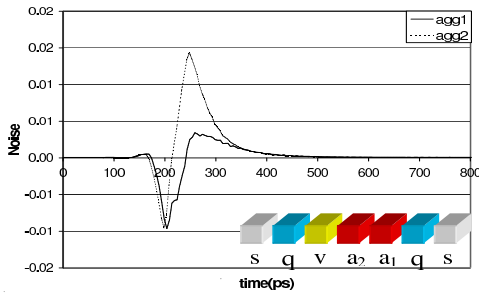


Fig. 3. noises on the victim caused by two aggressors in a five-bit $1000\mu\text{m}$ -long bus. The driver size is $30\times$, and the wire spacing is $1.7\mu\text{m}$.

TABLE II

NOISE PEAKS FOR A THREE-BIT $1000\mu\text{m}$ -LONG BUS STRUCTURES. THERE ARE TWO AGGRESSORS WHOSE SWITCHING PATTERNS ARE SHOWN INSIDE THE PARENTHESES IN THE LAST TWO COLUMNS

| bus | driver | spacing(um) | noise1(↑↑) | noise2(↓↓) |
|-------|------------|-------------|------------|------------|
| svaas | $30\times$ | 0.6 | 0.1323 | 0.1006 |
| svaas | $30\times$ | 1.6 | 0.0197 | 0.0229 |

3) *Impact of Routing Direction*: Signals are routed either from left (top) to right (down) or from right (down) to left (top). In figure 4, we present two signal nets in two different

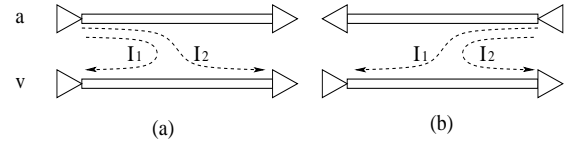


Fig. 4. Different routing patterns of two signal wires.

patterns of routing direction. One net is the victim and the other is the aggressor. The wires are aligned and the lengths are $1000\mu\text{m}$. We run SPICE simulations to study the noise of the two different settings. The noise on the victim is 0.1658 when the two nets routed in the same direction, but 0.2138 when they are routed in opposite directions. The difference between these two cases is 29%. This can be explained as follows: The different routing directions result in different current flow directions and in turn different loop inductances (see Figure 4), which results in large difference in the noise waveform even for a single aggressor. Therefore, the routing direction should be considered in the noise analysis under RLC model. In this work, we assume the routing direction is given, and the routing directions for all the signal nets are the same if not explicitly stated.

4) *WCN under RLC Interconnect Model*: In summary, we define the WCN problem under RLC model as follows:

Formulation 1: Given a non-switching victim and multiple aggressors in a pre-routed interconnect structure, find switching patterns and switching times for all aggressors such that the noise in the victim has maximal amplitude.

We will first study this problem without any timing window constraints in section III, and then study the problem with timing window constraints in section IV.

III. WCN WITHOUT TIMING CONSTRAINTS

In this section, we consider first the quiet victim without propagated noise from the previous stage and then the noisy victim with propagated noise from the previous stage.

A. Algorithms for Quiet Victim

1) *Extension to Existing Algorithms*: We extend *SS*, *SP* and *AS* by incorporating switching pattern generation as follows:

- *Simultaneous switching (SS)*: All aggressors switch simultaneously in the same direction. WCN is approximated by the maximum noise on the victim.
- *Superposition (SP)*: Find the maximum noise peak for each aggressor when only this aggressor switches. WCN is approximated by the sum of *amplitudes* (absolute values) of all such peaks.
- *Aligned switching (AS)*: Obtain *individual* noise waveform by simulating the interconnect structure with only one aggressor switching for each time, then simulate the circuit with multiple aggressors using the following switching times and patterns:
 - (i) *PP alignment*: align the maximum positive peaks of individual noise waveforms, and all aggressors switch in a same direction;

- (ii) *NN alignment*: align the maximum negative peaks of individual noise waveforms, and all aggressors switch in a same direction;
- (iii) *PN alignment*: align the peaks of maximum amplitude, and aggressors have switching directions such that all the aligned peaks have a same polarity.

WCN is approximated by the maximum noise among the above three simulations. Experiments have shown that none of the three kinds of alignments defined above is always better than the others, so all the three alignments are needed by *AS* algorithm.

2) *New Algorithms*: We propose the following *SS + AS* algorithm. In *SS + AS*, WCN is approximated by the larger one between the results obtained by *SS* and *AS*. The reason to combine *SS* and *AS* is that either *SS* or *AS* may produce a larger noise. To show this, we carry out experiments on an align bus structure with two aggressors and a victim, and show the results in Table III. From the table, *SS* produces 6% larger noise than *AS* in the first case but *AS* gives 1% larger noise than *SS* in the second case. As will be shown in the rest of this paper by the experiment results, *SS + AS* is a good approximation to WCN under RLC model.

TABLE III
NOISES OF *SS* AND *AS* IN DIFFERENT CASES

| length(μm) | driver | spacing(μm) | <i>SS</i> | <i>AS</i> |
|-------------------|-------------|--------------------|-----------|-----------|
| 500 | 50 \times | 0.6 | 0.173 | 0.163 |
| 2000 | 50 \times | 1.2 | 0.193 | 0.195 |

To validate the algorithms above, we also developed simulated annealing algorithm (*SA*) and genetic algorithm (*GA*) for the WCN problem under RLC model. We select the larger noise between the results from *SA* and *GA* as the accurate WCN. We call this algorithm as *SA + GA*. In *SA* algorithm, the value of the cost function is proportional to the maximal noise. There are two types of moves: 1. Adjust the arrival time of a randomly picked aggressor by a random factor from 0 to 10%; 2. Reverse the switching pattern of a randomly picked aggressor. We start the *SA* at an initial temperature of 50 and terminate it at 0.01. The temperature decreases by a factor of 0.9 and the number of moves at a particular temperature is equal to $100 \times n$, where n is the number of aggressors. For *GA* algorithm, each individual solution (*chromosome*) is encoded as an ordered array of aggressor switching time and switching pattern pairs. The population of each generation is equal to $4n$. The fitness of each individual is equal to the maximum noise on the victim. Two types of genetic operations are performed: 1. Crossover: produce offspring by exchanging parts of the settings of the aggressors between two parents; 2. Mutation: produce offspring by randomly changing the selected aggressors' switching time and switching pattern of a selected parent. The probability of a parent being selected is proportional to its fitness. The crossover and mutation probabilities are 0.5 and 0.3 respectively. The *GA* process terminates when there is no improvement for 20 continuous generations.

3) *Time Complexity*: In table IV, we compare the time complexity of different WCN algorithms under RLC model.

In the table, n is the number of aggressors. The estimated complexity of *SA + GA* is based on our experiments. We can see that *SS*, *SP*, *AS* and *SS + AS* all have a linear time complexity.

TABLE IV
TIME COMPLEXITY OF WCN ALGORITHMS FOR QUIET VICTIMS.

| Algorithm | Aggressor alignment | Time complexity |
|----------------|---|-----------------|
| <i>SS</i> | simultaneous switching | 1 |
| <i>SP</i> | sum of noise amplitude | n |
| <i>AS</i> | align three type of noise peak | $n + 3$ |
| <i>SS + AS</i> | simultaneous, align three type of noise peaks | $n + 4$ |
| <i>SA + GA</i> | simulated annealing and genetic algorithm | $\sim 20000n$ |

B. Experiments with Quiet Victim

We carry out a set of experiments with quiet victims in this section to validate our algorithms.

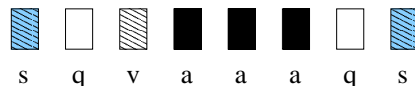


Fig. 5. Six-bit aligned bus with two shields

1) *Aligned Bus*: In this section we study the aligned six-bit coplanar bus structure as shown in Figure 5. We present the experiment results from different algorithms in table V. We take the results from *SA + GA* as accurate results. As shown in this table, *SS* and *AS* have an average underestimation less than 5% and the maximum underestimation is about 10% compared to *SA + GA*. Neither *SS* nor *AS* always produces larger noise than the other does. However, *SS + AS* gives results very close to *SA + GA*. The maximum underestimation of *SS + AS* is about 5% and the average underestimation is less than 3%. *SP* can underestimate up to 24% compared to *SA + GA*. WCN under RC model severely underestimates the noise in most cases, especially for strong drivers and larger spacing. The underestimation of applying RC model can be up to 80% compared to *SA + GA*.

2) *Different Routing Direction*: As discussed in section II-C, the routing direction impacts the WCN under RLC model significantly. Different routing directions result in different peak polarities or/and peak times, thus affect the alignment. Our alignment algorithm can automatically adjust the alignment shifting and polarity considering different routing directions. Therefore, all WCN algorithms are still valid for different routing directions.

We carry out a set of experiments using the six-bit aligned bus structure in Figure 5 but with different routing directions. The driver size is 150x, and the victim is quite. We present the experiment results in table VI. The two opposite directions are marked as '0' and '1' respectively. From the table, we can see *SS + AS* algorithm still achieves a high accuracy compared to *SA + GA* with an average error of 1% and a maximum error of 3%. When aggressors are routed in different directions, *SS* underestimates the WCN with an error much larger than

TABLE V
NOISES ON A QUIET VICTIM FROM DIFFERENT ALGORITHMS FOR ALIGNED RLC BUS STRUCTURE

| Driver | Spacing | RLC | | | | | RC |
|---------------|---------|-------|---------|--------|---------|--------|---------|
| | | SA+GA | SP | SS | AS | SS+AS | |
| 30× | 0.6 | 0.147 | 0.111 | 0.145 | 0.141 | 0.145 | 0.144 |
| 30× | 1.2 | 0.069 | 0.062 | 0.068 | 0.066 | 0.068 | 0.062 |
| 50× | 0.6 | 0.168 | 0.133 | 0.167 | 0.148 | 0.167 | 0.144 |
| 50× | 1.2 | 0.089 | 0.082 | 0.087 | 0.085 | 0.087 | 0.064 |
| 100× | 0.6 | 0.152 | 0.119 | 0.149 | 0.146 | 0.149 | 0.117 |
| 100× | 1.2 | 0.114 | 0.097 | 0.108 | 0.106 | 0.108 | 0.050 |
| 150× | 0.6 | 0.133 | 0.112 | 0.129 | 0.124 | 0.129 | 0.101 |
| 150× | 1.2 | 0.130 | 0.120 | 0.126 | 0.128 | 0.128 | 0.043 |
| 200× | 0.6 | 0.159 | 0.121 | 0.150 | 0.156 | 0.156 | 0.092 |
| 200× | 1.2 | 0.172 | 0.160 | 0.159 | 0.169 | 0.169 | 0.037 |
| Average Error | | 0.00% | -16.41% | -4.03% | -4.68% | -2.46% | -35.49% |
| Maximum Error | | 0.00% | -24.03% | -8.76% | -11.93% | -5.83% | -78.56% |

the errors with all aggressors routed in the same direction, because the skew between the maximum peaks of aggressors are larger with different routing directions. The *SP* algorithm underestimates or overestimates the WCN with errors up to 21%. The average of the absolute errors of *SP* is 12.07%. Therefore *SP* does not approximate WCN well.

3) *Unaligned Bus*: We conduct experiments on unaligned bus structures. Although shifting between aggressors in an unaligned bus structure can affect the timing of each aggressor, such impact is not significant due to the short flight time for on-chip interconnects. To show the effect, we calculate the flight time in a $1000\mu\text{m}$ long wire. We assume the dielectric is uniform, the relative dielectric constant is $\epsilon=3$, and the relative permeability is $\mu \approx 1$. The speed of light in such dielectric is $v = \frac{c}{\sqrt{\epsilon\mu}} \approx 1.7 \times 10^8 \text{m/s}$, where c is the speed of light in vacuum. For $1000 \mu\text{m}$ long wire, the flight time is $t_f \approx 6\text{ps}$. The flight time is relatively small compared to the signal rising time of 33ps assumed in our experiment, and should not significantly impact the quality of our WCN algorithms.

To verify our algorithms under general situations, we conduct the following experiments: We randomly select up to 50% of the wires to be shields and up to 90% of the rest of the wires to be aggressors, and randomly select one signal wire to be the victim. The wire length, spacing, driver size, shifting and routing direction are also randomly selected for each wire. The range of the parameters are summarized in Table VII. We study 100 cases and compare the noise values from *SS+AS* and *SA+GA* algorithms in Figure 6. From the figure we can see that compared to *SA+GA* algorithm our *SS+AS* algorithm is highly accurate with an average error of 2% and the maximum error less than 10%. In this experiment we randomly make up to 50% wires as shields, which are equivalent to power grids in the same layer of the bus. Since our algorithm achieves high accuracy in the experiments, we believe it can also be applied to more complex structure having multi-layer power grid with reasonable accuracy.

C. Noisy Victim

In this section, we consider noisy victims with noise propagated from the previous stage. We extend *SS*, *SP* and *AS* algorithms as follows:

- *Simultaneous Switching (SS)*: We assume all the aggressors switching simultaneously and in the same direction.

TABLE VII

PARAMETER RANGES FOR EXPERIMENTS OF UNALIGNED BUSES

| | |
|---------------------|------------------------|
| number of nets | 6-18 |
| wire length | 500-2000 μm |
| wire spacing | 0.6-1.8 μm |
| driver size | 50-200× |
| shifting | 0-0.8 wire length |
| dielectric constant | 2-3 |

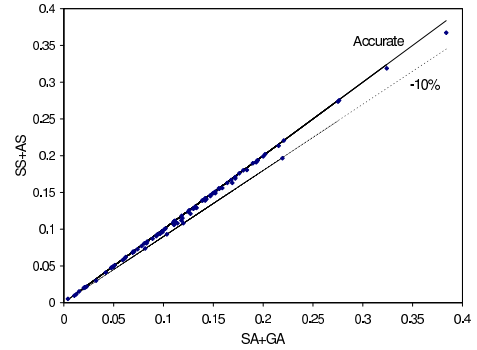


Fig. 6. SS+AS vs SA+GA

To find the proper switching time for the aggressors, we first find the maximum noise peak on the victim when all aggressors switch in the same direction simultaneously while the victim is quiet, and define this peak as the *aggressor-induced noise peak* (see Figure 7). Then we find the maximum peak of the propagated noise while all the aggressors are quiet, and define this peak as the *propagated noise peak* (see Figure 7). Finally we carry out a simulation with all the aggressors switching in the same direction and at the switching times such that the aggressor-induced noise peak and the propagated noise peak are aligned and they have the same polarity. The WCN is approximated by the maximum noise on the victim in this simulation.

- *Superposition (SP)*: We first find the peak noise value when only one aggressor switches and the victim is quiet. WCN is approximated by the sum of all such peak noise values and the peak value of the propagated noise.
- *Aligned Switching (AS)*: We first obtain individual noise waveform when only one aggressor switches, then carry

TABLE VI

NOISE ON A QUIET VICTIM WITH DIFFERENT ROUTING DIRECTIONS. THE AVERAGE ERROR FOR SP IS CALCULATED BASED ON THE ABSOLUTE DIFFERENCE OF NOISE.

| Direction s q v a a a q s | RLC | | | | | RC |
|------------------------------|-------|---------|---------|--------|--------|---------|
| | SA+GA | SP | SS | AS | SS+AS | |
| Space = 0.6 | | | | | | |
| 0 0 0 0 0 0 0 0 | 0.133 | 0.112 | 0.129 | 0.124 | 0.129 | 0.101 |
| 0 1 0 1 0 1 0 0 | 0.193 | 0.234 | 0.153 | 0.191 | 0.191 | 0.101 |
| 0 1 0 0 1 0 1 0 | 0.176 | 0.196 | 0.0775 | 0.176 | 0.176 | 0.101 |
| 0 0 0 1 1 1 0 0 | 0.200 | 0.172 | 0.199 | 0.198 | 0.199 | 0.101 |
| Space = 1.2 | | | | | | |
| 0 0 0 0 0 0 0 0 | 0.130 | 0.120 | 0.126 | 0.128 | 0.128 | 0.043 |
| 0 1 0 1 0 1 0 0 | 0.172 | 0.196 | 0.0902 | 0.171 | 0.171 | 0.043 |
| 0 1 0 0 1 0 1 0 | 0.152 | 0.166 | 0.0371 | 0.151 | 0.151 | 0.043 |
| 0 0 0 1 1 1 0 0 | 0.151 | 0.146 | 0.149 | 0.150 | 0.150 | 0.043 |
| Average Error | 0.00% | 12.07% | -25.97% | -1.53% | -1.00% | -56.13% |
| Maximum Error | 0.00% | +21.24% | -75.59% | -6.77% | -3.01% | -75.00% |

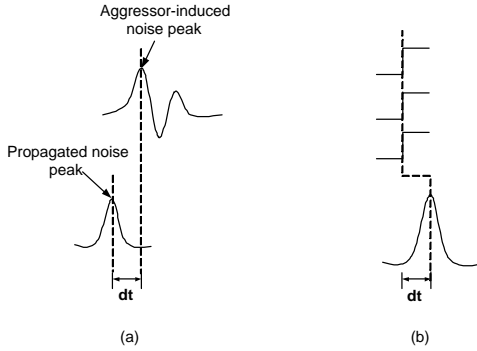


Fig. 7. Simultaneous switching algorithm with noisy victim. (a) aggressor-induced noise and propagated noise. (b) alignment.

out simulations with the three types of alignments defined in section III-A by treating the propagated noise as an individual noise waveform of an “extra” aggressor. WCN is approximated by the maximum noise among the three alignment procedures.

The $SS + AS$ algorithm for noisy victims can be readily extended using the above SS and AS algorithms. SA and GA can also consider the noisy victim by modeling the noise as a pseudo-aggressor. In table VIII, we summarize the time complexity for algorithms with noisy victims. We can see that the time complexity is almost the same as that of the corresponding algorithms for quiet victims.

TABLE VIII

TIME COMPLEXITY OF WCN ALGORITHMS FOR NOISY VICTIMS.

| Algorithm | Aggressor alignment | Time complexity |
|-----------|---|-----------------|
| SS | simultaneous switching | 3 |
| SP | sum of noise amplitude | $n + 1$ |
| AS | align three type of noise peaks | $n + 4$ |
| $SS + AS$ | simultaneous, align three type of noise peaks | $n + 5$ |
| $SA + GA$ | simulated annealing and genetic algorithm | $\sim 20000n$ |

We carry out experiments with the six-bit bus structure in Figure 5. We provide an artificial noise on the input of the driver to the victim. In table IX, we present the simulation results from different algorithms. We do not compare WCN

TABLE IX

NOISES ON A NOISY VICTIM FROM DIFFERENT ALGORITHMS FOR ALIGNED RLC BUS STRUCTURE

| Driver | Spacing | SA+GA | SP | SS | AS | SS+AS |
|---------------|---------|-------|---------|---------|--------|--------|
| 30 | 0.6 | 0.405 | 0.243 | 0.396 | 0.402 | 0.402 |
| 30 | 1.2 | 0.332 | 0.250 | 0.325 | 0.325 | 0.325 |
| 50 | 0.6 | 0.539 | 0.366 | 0.524 | 0.507 | 0.524 |
| 50 | 1.2 | 0.486 | 0.407 | 0.480 | 0.466 | 0.480 |
| 100 | 0.6 | 0.169 | 0.131 | 0.160 | 0.163 | 0.163 |
| 100 | 1.2 | 0.124 | 0.111 | 0.114 | 0.124 | 0.124 |
| 150 | 0.6 | 0.152 | 0.118 | 0.139 | 0.146 | 0.146 |
| 150 | 1.2 | 0.136 | 0.122 | 0.116 | 0.130 | 0.130 |
| 200 | 0.6 | 0.162 | 0.125 | 0.154 | 0.160 | 0.160 |
| 200 | 1.2 | 0.170 | 0.165 | 0.165 | 0.168 | 0.168 |
| Average Error | | 0.00% | -20.53% | -5.38% | -3.15% | -2.27% |
| Maximum Error | | 0.00% | -39.39% | -14.84% | -5.85% | -4.62% |

under RC with RLC models, because in previous section we have verified that RC model leads to large underestimation for WCN of multi-gigahertz interconnects. As shown in table IX, compared to $SA+GA$, the maximum underestimation of $SS+AS$ is 4.62%, and the average underestimation is 2.27%. It is again a very close approximation to $SA + GA$. SP severely underestimates WCN, with a maximum underestimation of 39.93% and an average underestimation of 20.53%.

IV. WCN PROBLEM WITH TIMING WINDOW CONSTRAINTS

In previous sections, we ignore the timing window constraints of aggressors and victim. In real design practice, there is a switching timing window for each aggressor. The switching timing window is the time interval between the earliest and latest switching times of the aggressor. For the victim, there is a sampling window at the input of its receiver. The sampling timing window is the time interval between the earliest setup time and the latest hold time of the flip-flop at the far end. It has been shown that considering timing window constraints can greatly reduce the number of false violations under RC model [14]. In this section, we extend our WCN algorithms to consider the timing window constraints for both aggressors and the victim.

A. Algorithm

To find the WCN under timing window constraints, we extend our algorithms in section II-C. We still consider three

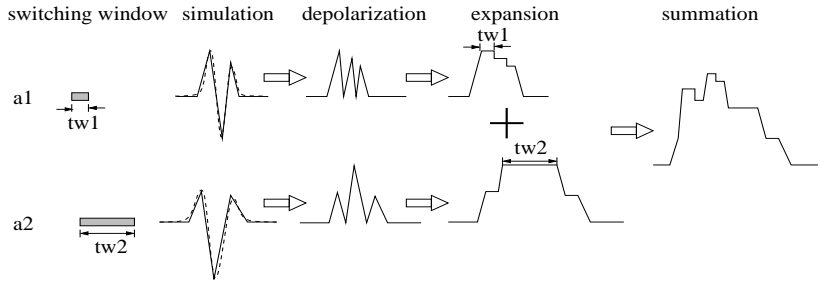


Fig. 8. PN alignment with timing windows

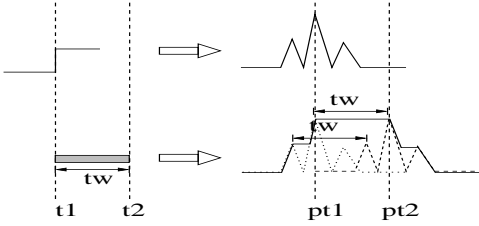


Fig. 9. Expansion of noise waveform

kinds of alignment: PP, NN and PN alignments. We first discuss PN alignment, where we align the aggressors according to the absolute maximum peak of each aggressor. As shown in Figure 8, the specific steps in PN alignment include:

(1) Simulation: We simulate the bus with one aggressor switching each time to obtain the individual noise waveform on the victim for each aggressor, and then for each individual noise waveform, we approximate the waveform by a piece-wise linear waveform which consists peak-to-peak straight lines. Because of the oscillation of the noise waveform in RLC circuits, normally the peaks are narrow and sharp and the linear model approximates the waveform very well for the purpose of WCN problem.

(2) Depolarization: We construct a new waveform which is the absolute value of the original piece-wise linear waveform.

(3) Expansion: We expand the waveform according to the aggressor's timing window. The expansion procedure is shown in figure 9. In this example there is one aggressor with switching timing window of $tw = t2 - t1$. During the expansion, we first expand each noise peak by tw , and then find the contour of all expanded peaks (i.e., the largest values at each time point). We record the peak polarity and switching timing of each region so that we can obtain the switching pattern and switching time of the aggressor later.

(4) Summation: To consider the noise contributions from all the aggressors, we sum up the waveform contours of all the aggressors to get an overall waveform contour. We find the time region with the maximum noise value in the waveform within the sampling window of the victim and the correspondent switching pattern and switching time of each aggressor. Finally, we carry out one-time simulation with the determined switching pattern and time, and use the max noise from this last simulation as WCN. We summarize the algorithm in table X.

The algorithms for PP and NN alignment with timing

TABLE X

STEPS TO DETERMINE THE WCN WITH TIME WINDOW CONSTRAINT

| | |
|---------|---|
| Step 1: | Simulation For each aggressor simulate with only the aggressor switching and others quiet. Proximate the noise waveform by piece-wise linear waveform for each aggressor. |
| Step 2: | Depolarization Obtain the waveform with the absolute value of the original waveform for each aggressor. |
| Step 3: | Expansion Expand each waveform peak by the width of the timing window and obtain the contour of the expanded waveform. |
| Step 4: | Summation Sum the contour waveforms in Step 3 for all the aggressors. Find the switching pattern and switching time that generate the maximal noise in the accumulated waveform within the sampling window of the victim. Simulate with the determined switching pattern and switching time to obtain WCN. |

window constraints are similar. Because in these two alignments all the aggressors have the same switching pattern, we may not need to change the polarity of noise by changing the switching pattern. Therefore, we do not need to use the absolute value of the waveform but instead use the original waveform. In the step of expansion, for PP alignment we get the largest noise (most positive) for the waveform contour, and for NN alignment we get the smallest noise (most negative) for waveform contour. The remaining steps are the same as those in PN alignment. The time complexity for alignment switching is $n + 3$ because we need n individual simulations for each aggressor and one simulation for each type of alignment.

We also extend the *SS* algorithm to consider the timing window constraints. We first determine all the overlapped regions for the timing windows of all the aggressors. For each of such regions, we find all the aggressors that can switch in the region, and find the simultaneous switching noise of those aggressors within the sampling window of the victim. The largest noise among the simultaneous switching noises of all the overlapped regions is the WCN. The time complexity of *SS* algorithm is $2n - 1$, where n is the number of aggressors, because each switching window has two ends and thus there are at most $2n - 1$ overlapped regions. For each overlapped region, one simulation is required, so the worst case is $2n - 1$.

After we obtain the maximal noise values from *AS* and *SS*, the *AS + SS* algorithm approximate the WCN by the larger one of the two. The worst-case time complexity of *AS + SS* with timing window constraints is $3n + 2$, the sum of the

runtime for *AS* and *SS*.

B. Experiments

To verify our algorithms, we carry out a set of experiments to compare *SS* + *AS* algorithm with *GA* + *SA* algorithm. In this set of experiments, the timing windows and routing directions are randomly generated for both the victim and the aggressors. We carry out the experiments on the aligned bus structure shown in Figure 5. The driver size is 100x and the victim is quiet. We summarize the experiment results in table XI. We do not compare the *SP* algorithm because it is meaningless to sum the maximum peaks without considering the timing windows. From the results, we can see that *SS*+*AS* approximates WCN very well with an average error of 2% and a maximum error of 5%. In this set of experiments, the *SS* algorithm generally behaves worse than the *AS* algorithm due to time window constraints of both the aggressors and the victim. However, with certain settings *SS* still can obtain larger noise than *AS* as shown in table XI. In table XI, we also present the WCN without the timing window constraints but with the same bus configurations. We can see that the WCN with timing window constraints can be up to 75% smaller than its peer without the timing window constraints. Thus, timing window constraints must be considered in WCN analysis to reduce false crosstalk violations.

Furthermore, we compare WCN under the RLC and RC models, both with timing window constraints. We use the WCN algorithm from [3] for the RC model. We use the aligned bus structure in Figure 5 with $0.6\mu\text{m}$ wire spacing and routing directions of “01010100” (“0” and “1” represent two opposite directions respectively). The centers of the aggressor switching windows are fixed and decided such that their maximal noise peaks under RLC model are perfectly aligned. In the experiments, we change the position of the victim sampling window and compute the correspondent WCN. In Figure 10, we show examples with a fixed driver size of $120\times$ but with different timing window sizes. From (a) to (c) in the figure, the sizes of the aggressor switching windows are 20ps, 30ps and 50ps respectively and the size of victim sampling window is 10ps, 15ps and 25ps respectively. The X-axis is the position of the victim sampling window center and the original point is the position that has the maximum WCN without the sampling window constraint. Clearly, the WCN under RLC model is much larger than that under RC model when there is no sampling window constraint. When there is a sampling window constraint, the WCN varies with respect to the position of the sampling window, and the RLC model still gives larger WCN than RC model in most cases.

However, in the circled parts of Figure 10(a) and 10(b), RC model produces larger WCN than RLC model does. Because of resonance in the noise waveform, the noise peaks are normally narrower and sharper under RLC model than under RC model, and thus the WCN of RLC model may be smaller than that of RC model when the sampling window is between two adjacent noise peaks in RLC model. When we increase the size of the timing windows as shown in Figure 10(b) and 10(c), the width of the peak increases and the adjacent peaks

from RLC model most likely overlap with each other. We can see that the overestimation of RC model gradually vanishes and the region of the overestimation moves away from the origin when the timing window sizes increase. When the sizes of timing windows are large enough, the overestimation of RC model disappears (see figure 10(c)). Overall, RC interconnect model underestimates the WCN in most cases, but it does overestimate the WCN when the timing window sizes are small enough. Whether RC model underestimates or overestimates the WCN depends on the detailed settings of the interconnects and the sizes and locations of the timing windows. We plan to develop efficient metrics to determine the conditions of RC model overestimating WCN in our future work. The underestimation under RC model leads to underdesign which causes circuit failures due to crosstalk violations, and the overestimation under RC model leads to overdesign which causes larger cost. For accurately analyzing the WCN problem of high-speed interconnects, the RLC model is necessary.

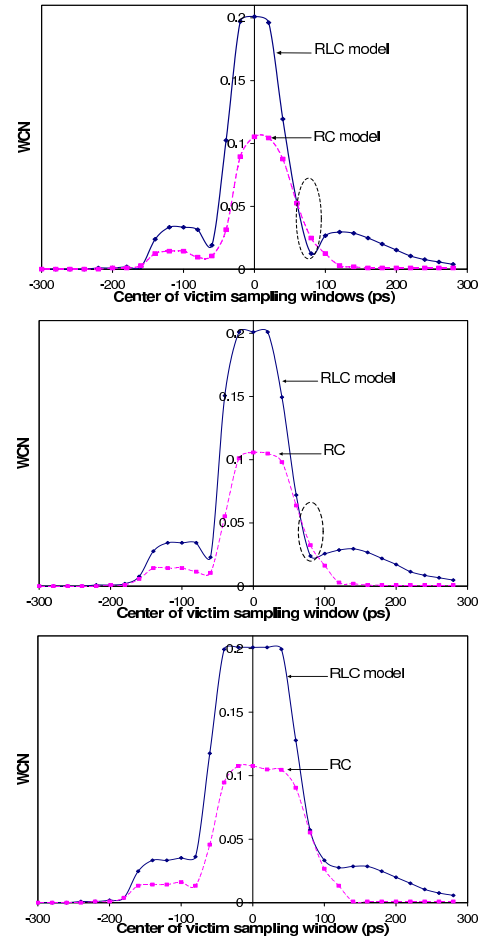


Fig. 10. WCN changes with the position of victim sampling window under RLC and RC models. Driver size is $120\times$.

V. CONCLUSION

Previous work has only studied interconnect worst case crosstalk noise (WCN) under RC model. In this work, we have presented the first in-depth study on WCN under RLC model

TABLE XI
NOISES ON A QUIET VICTIM WITH DIFFERENT TIMING WINDOWS

| Routing Direction s q v a a a q s | Timing Window (t_{start}, t_{end}) (ps) | | | | Noise | | | | WCN(No window) |
|--------------------------------------|---|------------|------------|-----------|--------|---------|---------|--------|----------------|
| | v | a1 | a2 | a3 | SA+GA | SS | AS | SS+AS | |
| Spacing = 0.6 μm | | | | | | | | | |
| 0 0 0 0 0 1 0 0 | (300,325) | (100, 200) | (100, 275) | (50,150) | 0.118 | 0.112 | 0.105 | 0.112 | 0.163 |
| 0 1 0 1 0 1 0 0 | (300,350) | (0, 200) | (150, 350) | (50,250) | 0.164 | 0.162 | 0.163 | 0.163 | 0.174 |
| 0 1 0 0 1 0 1 0 | (350,400) | (50, 250) | (100, 350) | (300,600) | 0.156 | 0.134 | 0.155 | 0.155 | 0.171 |
| 0 0 0 1 1 1 0 0 | (350,400) | (250, 450) | (100, 300) | (0,200) | 0.0510 | 0.0506 | 0.0510 | 0.0510 | 0.195 |
| Spacing = 1.2 μm | | | | | | | | | |
| 0 0 0 0 0 1 0 0 | (300,325) | (100, 200) | (100, 275) | (50,150) | 0.0705 | 0.0371 | 0.0695 | 0.0695 | 0.131 |
| 0 1 0 1 0 1 0 0 | (300,350) | (0, 200) | (150, 350) | (50,250) | 0.127 | 0.118 | 0.121 | 0.121 | 0.143 |
| 0 1 0 0 1 0 1 0 | (350,400) | (50, 250) | (100, 350) | (300,600) | 0.110 | 0.0608 | 0.109 | 0.109 | 0.133 |
| 0 0 0 1 1 1 0 0 | (350,400) | (250, 450) | (100, 300) | (0,200) | 0.0492 | 0.0481 | 0.0489 | 0.0489 | 0.137 |
| Average Error | | | | | 0.00% | -14.42% | -2.49% | -1.90% | +79.25% |
| Maximum Error | | | | | 0.00% | -47.38% | -11.02% | -5.09% | +178.46% |

with consideration of timing window constraints. We have shown that both switching time and switching logic pattern of aggressors affect the WCN under RLC model and the routing direction also impacts WCN significantly under RLC model. We have proposed a new $SS + AS$ algorithm, which has a linear time complexity, considers routing direction, and is applicable to the cases with or without timing constraints on the victim sampling windows and aggressor switching window. When there are no timing constraints, experiments have shown that the $SS + AS$ algorithm has an average underestimation of 3% and a maximum underestimation of 10%. In contrast, the commonly used superposition algorithm leads to an average underestimation of 15% and a maximum underestimation of 24%. In addition, applying RC model for interconnects in the predicted ITRS 0.10 μm technology underestimates WCN by up to 80%. When there are timing constraints, experiments have shown that the $SS + AS$ still well approximates WCN with an average underestimation of 2% and an maximum underestimation of 5%. Although RC model underestimates WCN in most cases with timing constraints, it *does* overestimate WCN when both the aggressor switching window and victim sampling window are small enough.

We have studied WCN for the quiet and noisy victim, but not a switching victim. Aggressors primarily affect the delay of the switching victim, and we will study the worst-case delay problem for the switching victim in the future. Furthermore, we plan to develop effective matrices determining when the accurate RLC noise model is needed and when more efficient RC noise models can be applied without jeopardizing signal integrity. We also intend to study the impact of routing direction on the RC noise, and integrate our WCN model with static timing analysis.

REFERENCES

- [1] P. D. Gross, R. Arunachalam, K. Rajagopal, and L. T. Pileggi, "Determination of worst-case aggressor alignment for delay calculation," in *Proc. Int. Conf. on Computer Aided Design*, 1998.
- [2] S. H. Choi, F. Dartu, and K. Roy, "Timed pattern generation for noise-on-delay calculation," in *Proc. Design Automation Conf*, 2002.
- [3] L. H. Chen and M. Marek-Sadowska, "Aggressor alignment for worst-case crosstalk noise," *IEEE Trans. on Computer-Aided Design of Integrated Circuits and Systems*, vol. 20, no. 5, pp. 612 – 621, May 2001.
- [4] L. He and K. M. Lepak, "Simultaneous shielding insertion and net ordering for capacitive and inductive coupling minimization," in *Proc. Int. Symp. on Physical Design*, 2000.
- [5] C. K. Cheng, L. Lillis, S. Lin, and N. Chang, *Interconnect analysis and synthesis*. John Wiley & Sons, Inc., 1999.

- [6] <http://www-device.EECS.Berkeley.EDU/pdm/>.
- [7] J. K. Ousterhout, "Switch-level delay models for digital MOS VLSI," in *Proc. Design Automation Conf*, 1984, pp. 542–548.
- [8] F. Dartu, N. Menezes, J. Qian, and L. T. Pileggi, "A gate-delay model for high-speed CMOS circuits," in *Proc. Design Automation Conf*, 1994, pp. 576–580.
- [9] M. Xu and L. He, "An efficient model for frequency-dependent on-chip inductance," in *Great Lakes Symposium on VLSI*, 2001.
- [10] N. H. E. Weste and K. Eshraghian, *Principles of CMOS VLSI Design: a Systems Perspective*, 2nd ed. Addison-Wesley, 1993.
- [11] L. He, N. Chang, S. Lin, and O. S. Nakagawa, "An efficient inductance modeling for on-chip interconnects," in *Proc. IEEE Custom Integrated Circuits Conference*, May 1999, pp. 457–460.
- [12] M. W. Beattie and L. Pileggi, "IC analyses including extracted inductance model," in *Proc. Design Automation Conf*, 1999.
- [13] Y. Cao, C. M. Hu, X. Huang, A. B. Kahng, S. Muddu, D. Stroobandt, and D. Sylvester, "Effects of global interconnect optimizations on performance estimation of deep submicron design," in *Proc. Int. Conf. on Computer Aided Design*, 2000.
- [14] K. Tseng and V. Kariat, "Static noise analysis with noise windows," in *Proc. Design Automation Conf*, 2003.